

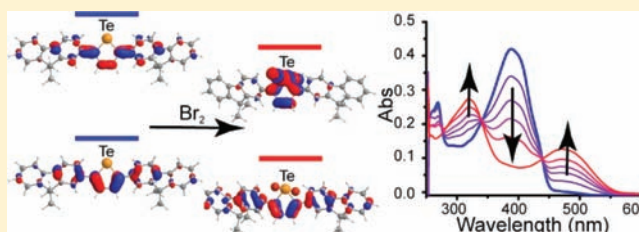
Tellurophenes with Delocalized π -Systems and Their Extended Valence Adducts

Theresa M. McCormick, Ashlee A. Jahnke, Alan J. Lough, and Dwight S. Seferos*

Department of Chemistry, University of Toronto, 80 St. George Street, Toronto, Ontario, M5S 3H6 Canada

S Supporting Information

ABSTRACT: The π -conjugated 2,5-substituted tellurophene compounds 2,5-bis(2-(9,9-dihexylfluorene))tellurophene (**1**) and 2,5-diphenyltellurophene (**3**) were synthesized through ring closing reactions of 1,4-substituted butadiyne. The oxidative addition of Br_2 to tellurophene compounds **1** and **3** was studied through absorption spectroscopy, NMR, electrochemistry, X-ray crystallography, and density functional theory (DFT) calculations. When Br_2 adds to the tellurium center the absorption spectrum shifts to a lower energy. From electrochemistry and DFT calculations we show that this is caused by lowering the lowest unoccupied orbital. The highest occupied orbital is also lowered, but to a lesser extent. This shift in absorption spectrum and lowering of the oxidation potential can provide a method to modify tellurophene containing materials. The two-electron oxidative addition is promising for catalyzing energy storage reactions.



INTRODUCTION

The metalloid tellurium is a versatile element that forms the basis for several important materials, including catalysts, dyes, and optoelectronic compounds.^{1–10} Tellurophene, the tellurium analog of the widely studied five-member heterocycle thiophene, however has not been extensively explored. This is particularly true of tellurophene-containing π -conjugated materials, even though they have certain advantages relative to their lighter analogs due to the unique chemistry of tellurium. These advantages include red-shifted optical absorption properties,^{11–13} unique solid-state supramolecular structures through tellurium–tellurium interactions,^{14–16} and high polarizability.^{17,18}

As research in π -conjugated materials has turned to more complex delocalized π -systems, and hence more lengthy synthetic pathways, there is a need to develop materials with properties that can be tuned postsynthesis. Examples of postsynthesis modification include complexation to form Lewis acid adducts,^{19–21} metal ion coordination,^{22–24} deprotonation at acid sites,²⁵ or ion exchange reactions.^{26,27} Tellurophene-containing π -conjugated materials are important in this regard as well, because of the diverse chemistry of this heteroatom. For example, tellurophenes (or similar tellurium-containing heterocycles) can extend their valence to form stable, isolatable, coordinated intermediates through oxidative addition reactions.²⁸

Recently, we described the synthesis of a novel, bifunctional tellurophene monomer, as well as the conditions required to prepare polytellurophenes by palladium-catalyzed solution-based methods.²⁹ This synthesis prepares well-defined polytellurophenes that are stable, processable materials. Interestingly, we observed a dramatic shift in optical properties

when these compounds were exposed to Br_2 , which appears to be the result of Br_2 coordination at their tellurium centers. The observed change in absorption properties of the tellurophene polymer upon exposure to Br_2 suggests a change in electronic distribution in the polymer, a property that could have several applications and advantages. Moreover, this shows that a single well-defined tellurophene compound can serve as an intermediate to produce a plurality of optoelectronic compounds. Specifically, through molecular engineering we can design and alter low energy sites in the polymer through specific chemical reactions. The reversible, two-electron oxidative addition reactions of X_2 at the tellurium center are especially important due to the potential use in energy storage reactions such as conversion of HX to H_2 and X_2 .^{30–33}

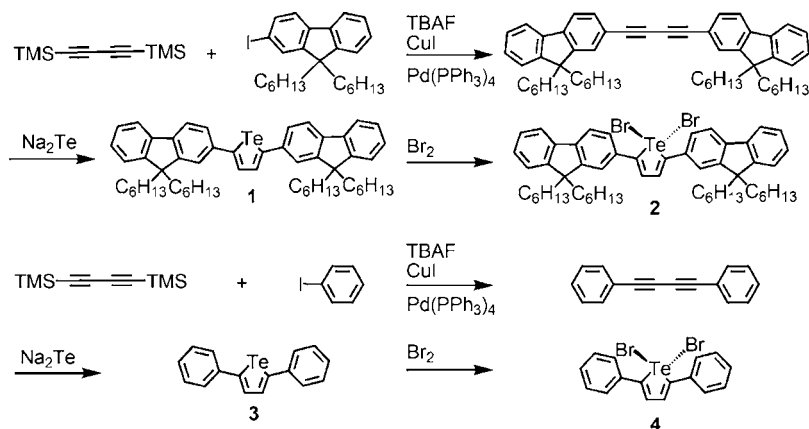
Herein, we present the first detailed investigation of the optoelectronic properties of tellurophene-based small molecules with extended π -systems and their extended valence adducts. Using carefully designed and synthesized tellurophenes, we fully characterize the structural, crystallographic, and optoelectronic properties of these compounds and their Br_2 adducts. By combining experimental results, density functional theory (DFT) calculations, and time-dependent DFT calculations we are able to discover the origin of the shift in optical and electronic properties of this new class of optoelectronic materials.

RESULTS AND DISCUSSION

Molecular Design and Synthesis. To understand both the electronic and structural basis for the change in optical

Received: November 29, 2011

Published: January 27, 2012

Scheme 1. Synthetic Route to Compounds 1–4^a

^aTMS is trimethylsilyl; TBAF is tetrabutylammonium fluoride.

properties when tellurophenes with delocalized π -systems coordinate with bromine, two compounds were synthesized and their Br_2 adducts were prepared. One compound is designed with an extended delocalized π -system 2,5-bis(2-(9,9-dihexylfluorene))tellurophene (**1**). The known compound 2,5-diphenyl-tellurophene (**3**)^{34–37} was also used for ease of crystallization to verify the geometry of bromine addition to the tellurium center. Importantly, the 2,5-substituted tellurophenes **1** and **3** can be accessed through functionalized butadiyne precursors, reacted with sodium telluride, allowing for a straightforward convergent synthesis (Scheme 1). The synthesis begins with the deprotection of bis(trimethylsilyl)-butadiyne by treatment with tetrabutylammonium fluoride in the presence of CuI and $\text{Pd}(\text{PPh}_3)_4$ and subsequent addition of an aryl iodide precursor to afford the desired 1,4-substituted butadiyne.³⁸ Sodium telluride was prepared³⁹ in refluxing ethanol by the slow addition of sodium borohydride to tellurium powder until the solution changed from a gray suspension, to purple, and finally a colorless solution. To afford the ring-closed tellurophene target compounds, a *tert*-butanol solution of 1,4-substituted butadiyne was added to the solution of sodium telluride followed by isolation and purification by column chromatography.

This synthetic pathway is important because the ring closing reaction^{40,41} and the formation of tellurophene occur in the final step, avoiding functionalization of the tellurophene ring, which can degrade under harsh reaction conditions. Purification by silica gel chromatography afforded the products in reasonable yields (11–55%) and in high purity. The tellurophene–dibromide adducts (**2** and **4**) were then prepared by the addition of 1 equiv of Br_2 to a carbon tetrachloride solution of the parent compounds. The composition of all products were verified by ^1H and ^{13}C NMR and high-resolution mass-spectrometry or elemental analysis (see the Experimental Section).

To examine the coordination of bromine to the tellurium center the structure of 2,5-bis(phenyl)dibromotellurophene (**4**) was determined by X-ray crystallography. X-ray quality crystals form as red blocks when methanol is allowed to slowly diffuse into a dichloromethane solution containing **4** (Figure 1). The structure reveals that two molecules of **4** (**4A** and **4B**) crystallize in each unit cell. The largest difference between the two molecules is the dihedral angle between the tellurophene and phenyl rings, which are 160.9° and 161.1° , and 174.4° and

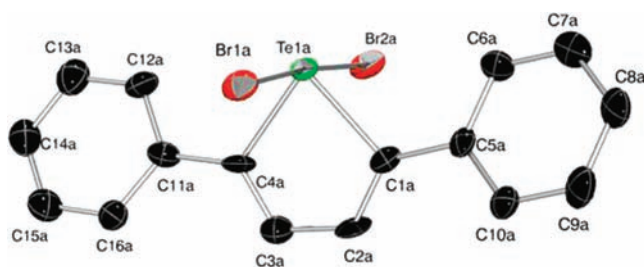


Figure 1. ORTEP drawing of compound **4** shown at 50% probability with hydrogens removed for clarity.

151.5° for **4A** and **4B**, respectively (see Supporting Information). This appears to be caused by solid state interactions of the phenyl rings. In the structure, we observe a seesaw configuration around the tellurium, the average $\text{Te}-\text{Br}$ bond length is 2.673 \AA , and the bond angle is $175.33(5)^\circ$. Due to the five-member ring the $\text{C}-\text{Te}-\text{C}$ bond angle in compound **4** is $82.0(5)^\circ$. The tellurophene ring has an average $\text{Te}-\text{C}$ bond length of 2.12 \AA , which is slightly longer than that of previously reported tellurophene compounds where the tellurium is not coordinated to bromine.⁴² A similar change is observed in the $\text{C}-\text{C}$ bond lengths. The $\text{C}2-\text{C}3$ average bond length is 1.33 \AA , decreased slightly from that of previously reported non-brominated compounds. While the $\text{C}3-\text{C}4$ length is increased to $1.46(2) \text{ \AA}$, indicating a significant degree of bond alternation in the ring, it is representative of a decrease in aromaticity compared to previously reported nonbrominated tellurophene compounds, and an increase in $\text{Te}-\text{C}$ bond length.

The conversion of **1** to **2** can be monitored by NMR. The single peak from the protons on the 3 and 4 position of the tellurophene shifts from 7.99 ppm in **1** to 7.55 ppm in compound **2** (Figure 2). This decreasing value of the resonance peak indicates that the tellurophene ring in **1** is more deshielded than **2**, which is also consistent with a loss of aromaticity when **1** is converted to **2**. When fractions of molar equivalents of Br_2 are added, NMR shows a clean conversion from **1** to **2** with no peak broadening. The integration of the peak at 7.99 ppm (0.75) and the doublet at 7.95 ppm (0.25) correlate to the amount of Br_2 added, supporting a 1:1 addition of Br_2 to compound **1**.

Optoelectronic Properties. With the structure upon Br_2 addition determined, the effect on the electronic properties was investigated. For these studies, we focused on compounds **1**

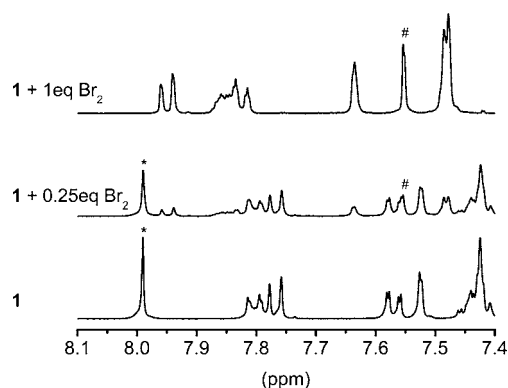


Figure 2. In the aromatic region of the ^1H NMR spectra of compound **1**, compound **1** with 0.25 mol equiv of Br_2 and compound **1** with 1 mol equiv of Br_2 added, the proton on the tellurophene ring is shown with an * for compound **1** and with a # for compound **2**. The spectra were acquired in CCl_4 with benzene inserts.

and **2** because they have an extended π -system and optical properties that lie in the visible region. Accordingly, **1** has a strong absorption band at 390 nm ($\epsilon = 4.5 \times 10^4 \text{ L cm}^{-1} \text{ mol}^{-1}$). Upon slow conversion of **1** to **2** (by the addition of Br_2 in 0.2 mol equiv aliquots) the band at 390 nm decreases, and two new bands, one at 470 nm and one at 320 nm, appear (Figure 3). This absorption titration experiment reveals two

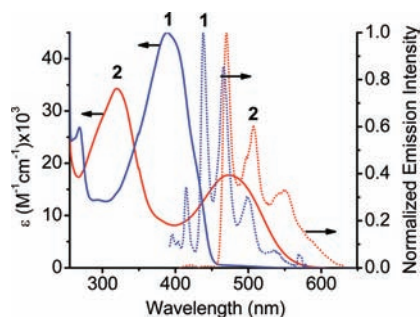


Figure 3. Absorption spectra of compounds **1** and **2** in dichloromethane at $1.3 \times 10^{-5} \text{ M}$ (solid lines). Normalized emission spectra of compounds **1** and **2** at 77 K in frozen 2-methyl-THF glass (dashed lines).

concurrent isosbestic points, showing a clean conversion of **1** to **2**. Two isosbestic points are observed because the starting compound has a single strong absorption and the product has two absorption bands. The reaction equilibrates after the addition of 1 equiv of Br_2 when the titration is carried out in a carbon tetrachloride solution (see Supporting Information). We also note that the dual band absorption appears to be characteristic of Br_2 -adducts **2** and **4** (see Supporting Information); its origin will be discussed in detail below.

Table 1. Experimental and Calculated Optical and Electrochemical Data (eV)

Compound ^a	$\text{Ox}_{\text{exp}}(\text{V})$	Ox_{cal}^d	$\text{Red}_{\text{exp}}(\text{V})^e$	$\text{Red}_{\text{cal}}^d$	$\text{Gap}_{\text{Echem}}^f$	$\text{Gap}_{\text{Optical}}^g$	$\text{Gap}_{\text{Calcd}}^h$
1	-5.70, -6.04 ^b	-5.08	—	-1.62	—	3.10	3.46
2	-6.20, -6.79 ^c	-5.58	-3.44	-2.79	2.76	2.46	2.79

^aStructures are given in Scheme 1. ^b $E_{1/2}$ from reversible oxidation peaks. ^c E_{ox} from maximum current of irreversible oxidation peak. ^dCalculated HOMO or LUMO energy level. ^e E_{red} from maximum current of irreversible reduction peak. ^fDifference of oxidation and reduction potentials. ^gOnset of low energy absorption band. ^hDifference between calculated HOMO and LUMO energy levels.

The effect of Br_2 addition on the photoluminescence properties of **1** and **2** was examined next. Emission from room temperature solutions of **1** and **2** is not observed, likely due to the presence of the heavy tellurium atom; however, frozen glasses of **1** and **2** in 2-methyl-THF (measured at 77 K) display vibrationally resolved luminescence (Figure 3). The heavy atom facilitates intersystem crossing to a triplet state; thus we hypothesize that the luminescence is phosphorescence since emission from these compounds is observed neither at room temperature nor in oxygenated solutions. At room temperature nonradiative decay pathways prevent emission. Likewise, triplet ground-state oxygen can cause deactivation of this state and quench emission. At 77 K the emission of compound **2** is red-shifted relative to compound **1**, which is consistent with the absorption spectra and a lower energy excited-state to ground-state transition for **2**, relative to **1**.

Next, cyclic voltametry was used to determine the positions of the frontier orbitals of these compounds; for clarity all values are reported vs vacuum (see Table 1). The energy of the HOMO level was experimentally found from the first oxidation peak. Compound **1** has reversible oxidizations at -5.70 V and -6.04 V. Both of these waves correspond to a one-electron oxidation with a nearly ideal peak splitting of 64 and 60 mV, respectively. Similar reversible oxidations are observed in other fluorene compounds with extended π -systems⁴³ but are not observed in tellurophene compounds including bitellurophene or tritellurophene⁴² and benzo[1,2-*b*:4,5-*b'*]ditellurophene.⁴⁴ This suggests that these waves are due to the oxidation of the extended π -system, rather than the metal center. No reduction peak was observed for **1**. Using the optical HOMO–LUMO gap of 3.10 eV, taken from the rise of the low energy absorption peak, the reduction should be near -2.6 V; this value is well beyond the electrochemical window of our experiments.

Unlike **1**, the oxidation of the brominated compound **2** is not reversible. The onset of oxidation occurs at -5.87 V. There is also a small oxidation shoulder at -6.20 V and an oxidation at -6.79 V. All of these values indicate that the HOMO of compound **2** is lower in energy than compound **1**. Additionally, compound **2** undergoes irreversible reduction at -3.04. Based on previous reports of halogenated tellurium-containing compounds, this first reduction peak is likely due to a debromination reaction.⁴⁵ Taking the optical HOMO–LUMO gap as the onset of absorption, the gap for **1** is 3.10 eV and for **2** is 2.46 eV. For compound **2**, taking the HOMO as the first oxidation potential and LUMO as the reduction potential the electrochemical energy gap is slightly larger at 2.79 eV (Table 1). The optical and electrochemical HOMO–LUMO gaps are in general agreement. Overall, this series of experiments has shown that both the HOMO and LUMO levels become more low-lying upon bromine addition.

■ COMPUTATIONAL STUDIES

To elucidate the electronic structure responsible for the observed optoelectronic properties, a series of DFT calculations were carried out. The geometries of compounds **1'**, **2'** (analogous to compounds **1** and **2** with methyl groups in place of the hexyl chains), 9,9-dimethylfluorene, tellurophene, and dibromotellurophene were optimized using the Gaussian 09 software package. All geometries were optimized to a minimum as verified by frequency calculations.

The extent of conjugation in **1'** was determined by comparing the electron density of the frontier orbitals with individual tellurophene and fluorene units. We will first describe the frontier orbitals of

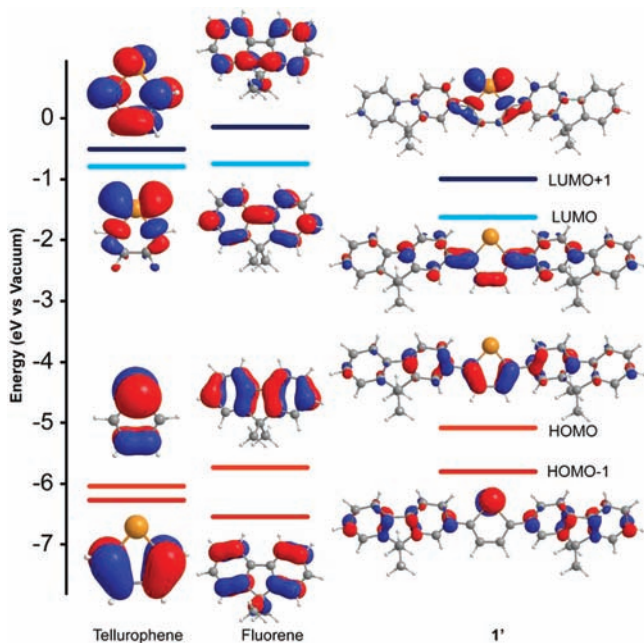


Figure 4. Calculated frontier orbitals of tellurophene, fluorene, and compound **1'** with an isocontour value of 0.05.

tellurophene and fluorene (Figure 4). The HOMO of tellurophene is π in nature with significant electron density on the tellurium atom and the carbons C3–C4. The LUMO of tellurophene has d-orbital character from the tellurium atom (Te_d), and the LUMO+1 is the first unoccupied π^* orbital. The HOMO and LUMO of 9,9-dimethylfluorene are delocalized π and π^* orbitals respectively. When tellurophene is coupled to 9,9-dimethylfluorene in the 2 and 5 positions (compound **1'**) the electron density is further delocalized over the entire π -system. This delocalization is supported by the narrowing of the calculated HOMO–LUMO gap for compound **1'** (the HOMO becomes higher in energy, and the LUMO becomes lower in energy) compared to tellurophene and 9,9-dimethylfluorene. Unlike the unsubstituted tellurophene, the HOMO of **1'** does not have electron density on the tellurium atom, and rather the electron density resides on the carbon atoms in the ring. In the HOMO–1, the electron density does reside on the tellurium atom. The LUMO for **1'** is a delocalized π^* orbital, and the LUMO+1 contains the tellurium d-character, which is switched in order compared to tellurophene.

When tellurophene is converted to the dibromine adduct both the HOMO and LUMO decrease in energy (Figure 5). The HOMO has electron density on the bromine atoms, with contribution from the p orbitals (Br_p). The LUMO is delocalized over the π -system and also includes Br_p orbitals. When dibromotellurophene is coupled to fluorene in the 2 and 5 positions (compound **2'**) the HOMO of the complex is a delocalized π orbital, similar in electron density distribution to compound **1'**, but destabilized by 0.51 eV. The LUMO of **2'**, however, is a tellurophene π^* orbital with contribution from the two Br_p orbitals, which resembles the LUMO of

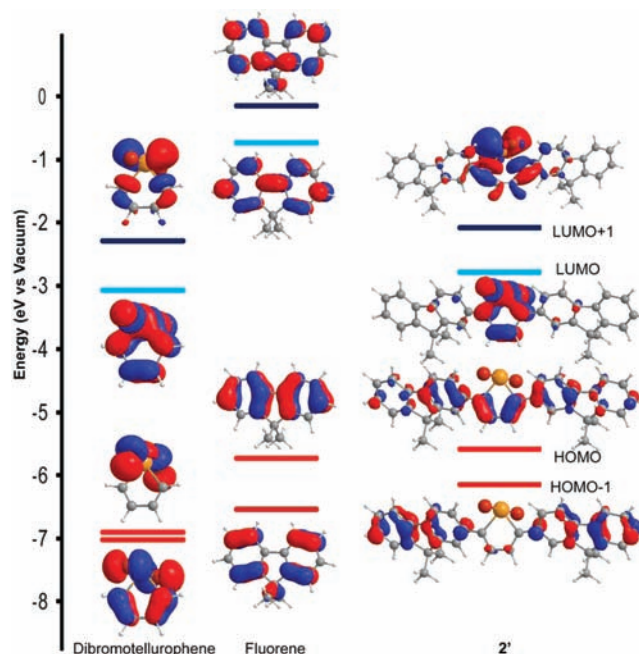


Figure 5. Calculated frontier orbitals of tellurophene, fluorene, and compound **1'** with an isocontour value of 0.05.

dibromotellurophene. The LUMO of **2'** is stabilized by 1.71 eV compared to compound **1'**, resulting in an overall smaller calculated HOMO–LUMO gap in **2'**. Taken together, these calculations indicate that the red shift in absorption upon bromination is at least partly a result of the involvement of the bromine atoms in the delocalized electronic structure, as well as a redistribution of electron density (discussed in detail below).

To understand optical absorption properties, time-dependent DFT (TD-DFT) calculations were carried out on both compounds **1'** and **2'**

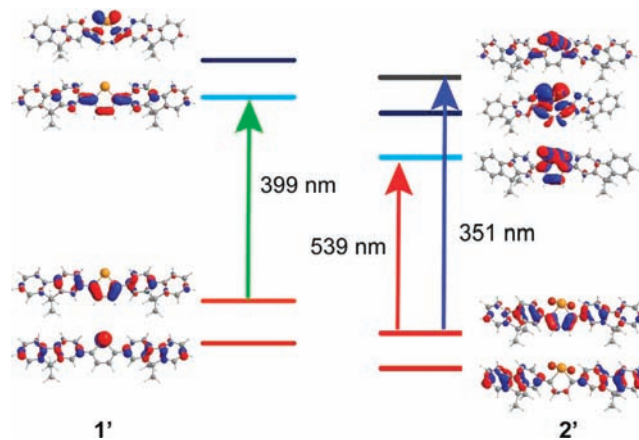


Figure 6. Calculated frontier orbitals of compounds **1** and **2** showing the calculated transitions.

(Figure 6). These calculations were then used to determine the orbitals involved in the transitions that make up the absorption spectra. The first 20 singlet and triplet states were calculated. For compound **1'** these calculations predict a state at 3.1 eV (399 nm, $f = 1.6$; where f is the oscillator strength of the transition, and a value over 0.1 is considered significant) consisting of a HOMO to LUMO transition involving the π and π^* orbitals. The single strong transition is consistent with the optical absorption spectrum of **1** (see Supporting Information).

The TD-DFT calculations for **2'** predict two states with high oscillator strengths, one low in energy (2.3 eV; 539 nm) and one high in energy (3.5 eV; 351 nm). The low energy state at 539 nm ($f = 0.44$) is a HOMO to LUMO transition involving the π and π^* -Br_p orbitals. The high energy state at 351 nm ($f = 1.02$) is mainly (90%) comprised of a HOMO to LUMO+2 transition, where the LUMO+2 involves the π^* orbital with a contribution from both the Te_p and Br_p orbitals. Just as in **1'**, the TD-DFT calculations on **2'** match the experimental absorption spectrum of **2**, which has peaks at 470 and 320 nm.

Overall, the unique features of the tellurophene compound **2** are the red-shift in optical properties, the low-lying HOMO and LUMO levels, and the dual band absorption profile. DFT calculations reveal that a large reorganization of the electron distribution occurs during the **1** to **2** transformation. In the HOMO, both compounds have a delocalized electronic structure as indicated by orbital contribution across the π -system of the entire molecule. In **1'** the LUMO is also very delocalized. In **2'**, however, the unoccupied orbitals appear to be much more localized on the tellurium ring. We postulate that this is similar to the formation of a ground-excited state charge transfer (C-T) complex. Indeed, previous work on polymers with charge-transfer π -systems has shown that they typically have narrow optical HOMO–LUMO gaps, dual bands in their absorption spectra, and low-lying frontier orbitals relative to π -systems that do not have a strong C-T.⁴⁶ Conversion of **1** to **2** engineers a discrete C-T in the π -system.

To gain insight into how the tellurophenes described herein differ from previous tellurium compounds, DFT and TD-DFT calculations were performed on a six member tellurium-containing heterocycle that exhibits a blue shift in absorption upon Br₂ addition, 4-[4-(dimethylamino) phenyl]-2,6-dimethyltelluropyrylium chloride (see Supporting Information).^{45,47–49} This telluropyrylium dye is cationic and contains two six-member rings, one containing tellurium, the other containing an amine group. Here, the parent (nonbrominated) compound has a HOMO that is delocalized throughout the π -system, including the p orbital of the tellurium atom, and a LUMO that is delocalized over the π^* -system. Conversion to the dibromine adduct stabilizes the HOMO; however this also excludes the tellurium from the π -system. This results in a disruption of the conjugation and causes a predicted blue shift in absorption properties, which matches the experimental data. The TD-DFT calculations show that the lowest energy singlet transition with a high oscillator strength is a transition from the HOMO to the LUMO for the parent compound (π – π^*) at 491 nm ($f = 0.88$). In the dibrominated compound, however, the first singlet state with a strong oscillator strength ($f = 0.80$) occurs at 458 nm with almost equal contributions from the HOMO to LUMO transition and HOMO–5 to LUMO transition, which is a π -Br_p and Br_p orbital to π^* orbital transition. The mixture of the low-lying Br_p orbitals results in the blue-shifted absorption spectrum of the dibromo adducts. Pertelluranes, five-member rings containing tellurium that is ionically bound to an oxygen in the ring, also exhibit a bathochromic shift in absorption upon bromination,^{50,51} which is due to a destabilization of the HOMO energy level.⁵²

CONCLUSIONS

Tellurophenes are a relatively unexplored class of compounds, particularly those with extended π -systems. Through the synthesis of 2,5-substituted tellurophene small molecules, 2,5-bis(2-(9,9-dihexylfluorene))tellurophene (**1**), and 2,5-diphenyl-tellurophene (**3**), as well as the Br₂ adducts **2** and **4**, we understand how the optical and electronic properties of tellurophenes with extended π -systems are controlled by the coordination environment at the tellurium center. Conversion of **1** to **2** changes the measured optical absorption spectrum and oxidation potential of the compound. Namely, compound **2** has a red shift in optical properties, more low-lying HOMO and LUMO levels, and dual as opposed to single absorption profile, when compared with **1**. Br₂ addition lowers the HOMO and as such is a potentially useful way to increase stability to oxidation, which is a concern for these types of heterocycles,

and also to modify optical and electronic properties by engineering discrete low-energy sites into the π -system. Due to their optoelectronic properties and reactivity, these novel compounds have potential use as semiconducting materials. Moreover, two-electron oxidative addition to tellurophenes is promising for catalyzing energy storage reactions. The relatively straightforward synthesis reported here should inspire researchers to begin to design and develop tellurophenes as catalysts as well as optoelectronic materials.

EXPERIMENTAL SECTION

General Considerations. All reagents were used as received unless otherwise noted. Tellurium, periodic acid dehydrate, potassium iodide (KI), bromohexane, bis(trimethylsilyl)butadiyne, palladium tetrakis(triphenylphosphine) (Pd(PPh₃)₄), tetrabutylammonium fluoride, and bromine were purchased from Sigma-Aldrich. Acetic acid, sulphuric acid, iodine, NaCO₃, MgSO₄, dichloromethane, hexanes, DMSO, KOH, and sodium thiosulfate were purchased from Fisher Scientific. Fluorene, CuI, sodium borohydride, and iodobenzene were purchased from Alfa Aesar. Silica gel was purchased from Silicycle.

The compounds 2-iodo-fluorene,⁵³ 2-iodo-9,9-dihexylfluorene,⁵⁴ and 2,5-bis(phenyl)tellurophene³⁵ were synthesized according to literature procedures with minor modifications as indicated below. The known compounds were characterized by ¹H NMR and were in agreement with literature.

Absorption spectra were recorded using a Varian Cary 5000 spectrometer. Emission spectra were recorded on a PTI fluorimeter with a photodiode detector and xenon arc lamp source. NMR spectra were recorded on a Varian Mercury 400 spectrometer (400 MHz). Masses were determined on a Waters GCT Premier ToF mass spectrometer (EI). Electrochemistry was performed with a BASi Epsilon potentiostat.

Computations. Calculations were performed using the Gaussian program,⁵⁵ utilizing DFT with the B3LYP level of theory.^{56,57} The basis set 6-31(d) was used for C and H atoms, and LAND2Z was used for tellurium and bromine atoms.⁵⁸ The structures were generated using Gausview 5.0 and optimized to a minimum. From the optimized geometry the first 20 singlet and triplet transitions were calculated using time-dependent DFT.⁵⁹

Cyclic Voltammetry. In 5 mL of dichloromethane, 5 mg of compound **1** or **2** were dissolved, along with 0.19 g of tetrabutylammonium hexafluorophosphate electrolyte. The working electrode was a 2 mm Pt-disk, the counter electrode was a Pt wire electrode, and the pseudoreference electrode was a Ag wire, with a ferrocene internal reference and a scan rate of 500 mV/s.

Titrations. A 1.3×10^{-5} M solution of **1** in CCl₄ was prepared and transferred to a 3 mL cuvette. A 1.95×10^{-4} M solution of Br₂ was added in 20 μ L aliquots, or 0.1 mol equiv. The absorption spectrum was recorded at each point after 5 min of stirring.

Synthesis. **2-Iodo-fluorene.**⁵³ Fluorene (10 g, 60 mmol) was dissolved in 100 mL of a boiling mixture of acetic acid, water, and sulphuric acid (100:20:3). The mixture was cooled to 65 °C, and periodic acid dehydrate (2.3 g, 10 mmol) and iodine (5.1 g, 20 mmol) were added. The red solution was stirred overnight, and upon cooling to room temperature a yellow solid was observed. Dichloromethane was added to dissolve the solid. The organic layer was washed with saturated NaHCO₃ solutions (3 \times 50 mL) and then dried with MgSO₄. The solvent was evaporated under reduced pressure. The resulting solid was recrystallized three times from hot hexanes (5.85 g, 30.2% yield). ¹H NMR (400 MHz, CDCl₃): δ 3.88 (s, 2H), 7.34 (m, 1H), 7.39 (m, 1H), 7.55 (m, 2H), 7.71 (m, 1H), 7.77 (m, 1H), 7.90 (m, 1H) ppm. Spectroscopy was identical to that of the previous report of this compound.

2-Iodo-9,9-dihexylfluorene.⁵⁴ A solution of 2-iodo-fluorene (1.7 g, 5.7 mmol) in DMSO was cooled in an ice bath and treated with KOH (0.92 g, 16 mmol) and KI (0.13 g, 7.7 mmol) to afford a red solution. After the KOH was fully dissolved, bromohexane (1.6 mL, 11 mmol)

was added, and the solution was allowed to warm to room temperature and stir overnight. The solution was extracted with dichloromethane and washed with a 10% solution of sodium thiosulfate, followed by brine and water. The organic layer was dried with MgSO_4 , and the solvent was removed under reduced pressure. Column chromatography (silica gel, hexanes) afforded the title compound as a yellow oil (1.9 g, 81% yield). ^1H (400 MHz, CDCl_3): δ 0.58–0.63 (m, 4H), 0.76 (t, $J = 6.75$ Hz, 6H), 1.04–1.16 (m, 12H), 1.90–1.96 (m, 4H), 7.31–7.38 (m, 3H), 7.44–7.46 (m, 1H), 7.64–7.69 (m, 1H). Spectroscopy was identical to that of the previous report of this compound.

1,4-Bis(2-(9,9-dihexylfluorene))buta-1,3-diyne. Bis(trimethylsilyl)butadiyne (0.10 g, 0.52 mmol), $\text{Pd}(\text{PPh}_3)_4$ (0.059 g, 0.052 mmol), CuI (0.019 g, 0.10 mmol), and 2-iodo-9,9-dihexylfluorene (0.50 g, 1.1 mmol) were added to a Schlenk bomb and degassed by three pump purge cycles. Dry, degassed toluene was added, followed by tetrabutylammonium fluoride (1.6 mL, 1 M in THF, 1.6 mmol). **CAUTION:** Diacetylene gas is formed and is flammable and can form explosive mixtures with air. Care should be taken with the deprotection of bis(trimethylsilyl)butadiyne. The reaction mixture turned deep red in color, was sealed and heated to 50 °C, and stirred overnight. The reaction mixture was diluted with dichloromethane and washed three times with brine, the organic layer was dried with MgSO_4 , and the solvent was removed under reduced pressure. Column chromatography (silica gel, hexanes) afforded a white solid (0.30 g, 80% yield). ^1H (400 MHz, CDCl_3): δ 0.61–0.64 (m, 4H), 0.79 (t, $J_1 = 7.1$ Hz, 6H), 1.04–1.16 (m, 12H), 1.97 (t, $J_1 = 8.3$ Hz, 4H), 7.34–7.36 (m, 3H), 7.53 (d, $J_1 = 1.7$ Hz, 1H), 7.54 (d, $J_1 = 1.4$ Hz, 1H), 7.67 (d, $J_1 = 8.4$ Hz, 1H), 7.71 (dd, $J_1 = 7.3$ Hz, $J_2 = 2.2$ Hz, 1H). ^{13}C NMR (CDCl_3 , 100 MHz): 13.0, 22.6, 23.7, 29.7, 31.5, 40.3, 55.1, 74.1, 83.1, 119.7, 119.9, 120.2, 122.9, 126.9, 126.9, 127.8, 131.5, 140.1, 142.3, 150.8, 151.2. TOF MS EI+ $\text{C}_{34}\text{H}_{66}$. Expected: 714.5165. Found: 714.5179. $\Delta = 2.0$ ppm.

2,5-Bis(2-(9,9-dihexylfluorene))tellurophene (1). Tellurium powder (71 mg, 0.56 mmol) was suspended in 10 mL of degassed ethanol. A sodium borohydride (0.20 g, 5.3 mmol) solution in 9:1 ethanol/water (50 mL) was slowly added to the refluxing tellurium suspension. After the solution turned from gray to purple to colorless a solution of 1,4-bis(2-(9,9-dihexylfluorene))buta-1,3-diyne (0.15 g, 0.27 mmol) in *n*-butanol (100 mL) was slowly added after the solution was cooled to 60 °C. The reaction was stirred overnight at 60 °C. The mixture was stirred under a flow of air for 20 min to oxidize the unreacted sodium telluride and filtered through Celite. The solvent was removed under reduced pressure. The residue was dissolved in dichloromethane and washed three times with brine. The organic layer was dried with MgSO_4 , and the solvent was removed under reduced pressure. Column chromatography (silica gel, hexanes) afforded a yellow powder (45 mg, 55% yield). ^1H (400 MHz, CDCl_3): δ 0.64–0.74 (m, 4H), 0.79 (t, $J_1 = 7.02$ Hz, 6H), 1.06–1.17 (m, 12H), 2.00 (t, $J_1 = 8.38$ Hz, 4H), 7.32–7.37 (m, 3H), 7.47–7.49 (m, 2H), 7.66–7.68 (m, 1H), 7.72 (dt, $J_1 = 7.0$ Hz, $J_2 = 1.2$ Hz, 1H), 7.93 (s, $J_{\text{Te}} = 20.3$ Hz, 1H). ^{13}C NMR (CDCl_3 , 100 MHz): δ 14.0, 22.6, 23.7, 29.7, 31.5, 40.4, 55.1, 119.7, 120.1, 120.6, 122.9, 126.2, 126.8, 127.1, 133.6, 138.8, 140.6, 140.9, 148.7, 151.0, 151.6. TOF MS EI+ $\text{C}_{54}\text{H}_{68}\text{Te}$. Expected: 864.4383. Found: 846.4407. $\Delta = 2.8$ ppm.

2,5-Bis(2-(9,9-dihexylfluorene))dibromotellurophene (2). 2,5-Bis(2-(9,9-dihexylfluorene))tellurophene (0.10 g, 0.12 mmol) was dissolved in 5 mL of CCl_4 . A solution of bromine (0.1 mL of Br_2 in 1.0 mL of CCl_4) was prepared, and 60 μL were added (0.12 mmol). The mixture was layered with methanol and refrigerated for 3 days to obtain red crystals collected by filtration (72% yield). ^1H (400 MHz, CDCl_3): δ 0.70 (m, $J = 8.38$ Hz, 4H), 0.78 (t, $J = 7.02$ Hz, 6H), 1.02–1.20 (m, 12H), 2.02 (dd, $J = 9.45$, 7.11 Hz, 4H), 7.35–7.41 (m, 3H), 7.49 (s, 1H), 7.55 (d, $J = 1.36$ Hz, 1H), 7.61 (dd, $J = 7.99$, 1.75 Hz, 1H), 7.75 (d, $J = 3.51$ Hz, 1H), 7.79 (d, $J = 7.80$ Hz, 1H). ^{13}C NMR (CDCl_3 , 100 MHz): δ 14.0, 22.5, 23.8, 29.6, 31.4, 40.2, 55.4, 120.3, 120.8, 121.49, 123.1, 127.1, 128.1, 131.5, 137.5, 139.8, 143.9, 151.4, 152.3, 163.1. CHN: $\text{C}_{54}\text{H}_{68}\text{TeBr}_2$. Expected: C, 64.57; H, 6.82. Found: C, 64.0; H, 6.73.

1,4-Bis(phenyl)buta-1,3-diyne. Bis(trimethylsilyl)butadiyne (0.84 g, 4.26 mmol), $\text{Pd}(\text{PPh}_3)_4$ (0.49 g, 0.43 mmol), CuI (0.16 g, 0.85

mmol), and iodobenzene (2.0 g, 9.8 mmol) were added to a Schlenk bomb and degassed by three pump purge cycles. Dry, degassed toluene was added (20 mL), followed by tetrabutylammonium fluoride (13 mL, 1 M in THF, 13 mmol). The reaction mixture turned deep red in color and was sealed, heated to 50 °C, and stirred overnight. The reaction mixture was diluted with dichloromethane and washed three times with brine. The organic layer was dried with MgSO_4 , and the solvent was removed under reduced pressure. Column chromatography (silica gel, hexanes) afforded the title compound, a white crystalline solid (0.18 g, 21% yield). ^1H (400 MHz, CDCl_3): δ 7.33–7.39 (m, 6H), 7.53–7.56 (m, 4H). ^{13}C NMR (CDCl_3 , 100 MHz): δ 73.9, 81.5, 121.8, 128.4, 129.2, 132.5. TOF MS EI+ $\text{C}_{16}\text{H}_{10}$. Expected: 202.0783. Found: 202.0784. $\Delta = 0.5$ ppm.

2,5-Bis(phenyl)tellurophene (3).³⁵ Tellurium powder (380 mg, 2.9 mmol) was suspended in 20 mL of degassed ethanol. A sodium borohydride (0.26 g, 6.9 mmol) solution in 9:1 ethanol/water (50 mL) was slowly added to the refluxing tellurium suspension. After the solution turned from gray to purple to colorless a solution of 1,4-bis(phenyl)buta-1,3-diyne (0.20 g, 0.98 mmol) in *n*-butanol (100 mL) was slowly added after the solution was cooled to 50 °C. The reaction was stirred overnight at 50 °C. The mixture was stirred under a flow of air for 20 min to oxidize the unreacted sodium telluride and filtered through Celite. The solvent was removed under reduced pressure. The residue was dissolved in dichloromethane and washed three times with brine. The organic layer was dried with MgSO_4 , and the solvent was removed under reduced pressure. Column chromatography (silica gel, hexanes) afforded the title compound, a light yellow crystalline solid (35 mg, 11% yield). ^1H (400 MHz, CDCl_3): δ 7.29–7.31 (m, 2H), 7.34–7.38 (m, 4H), 7.49–7.51 (m, 4H), 7.84 (s, $J_{\text{Te}} = 5.5$ Hz, 1H). ^{13}C NMR (CDCl_3 , 100 MHz): δ 126.7, 127.6, 129.0, 133.9, 139.9, 148.3. TOF MS EI+ $\text{C}_{54}\text{H}_{68}\text{Te}$. Expected: 335.00795. Found: 335.00902. $\Delta = 3.2$ ppm.

2,5-Bis(phenyl)dibromotellurophene (4). Compound 3 (8.0 mg, 0.024 mmol) was dissolved in 5 mL of CCl_4 . A solution of bromine (0.5 mL of Br_2 in 100 mL of CCl_4) was prepared, and 0.25 mL was added (0.024 mmol, 1 equiv). The mixture was layered with methanol and was refrigerated for 3 days. Orange-red plate crystals were collected and examined by single crystal X-ray diffraction (7.5 mg, 63.3% yield). ^1H (400 MHz, CDCl_3): δ 7.44 (s, $J_{\text{Te}} = 5.5$ Hz, 2H), 7.49–7.51 (m, 3H), 7.63–7.65 (m, 4H). ^{13}C NMR (CDCl_3 , 100 MHz): δ 126.3, 127.5, 128.2, 129.7, 130.7, 138.5. TOF MS EI+ $\text{C}_{16}\text{H}_{12}\text{TeBr}_2$. Expected: 412.91846. Found: 412.91826. $\Delta = 0.5$ ppm.

■ ASSOCIATED CONTENT

📄 Supporting Information

Crystal structure of 4, crystal data and structure refinement of compound 4, selected bond lengths and angles of compound 4, Stern–Volmer plot for the addition of Br_2 to 1, absorption spectrum of compounds 3 and 4, cyclic voltammogram for compounds 1 and 2, calculated and experimental absorption of 1 and 2, frontier orbitals for telluropyrillium dyes, geometry coordinates for optimized structures, and complete citation for ref 55. This material is available free of charge via the Internet at <http://pubs.acs.org>.

■ AUTHOR INFORMATION

Corresponding Author

dseferos@chem.utoronto.ca

Notes

The authors declare no competing financial interest.

■ ACKNOWLEDGMENTS

This work was supported by the University of Toronto, NSERC, the CFI and the Ontario Research Fund. We would like to thank Dmitry Pichugin and Marius Kapp for their help with the benzene insert NMR.

■ REFERENCES

- (1) Detty, M. R.; Luss, H. R. *Organometallics* **1986**, *5*, 2250–2256.
- (2) Leonard, K. A.; Zhou, F.; Detty, M. R. *Organometallics* **1996**, *15*, 4285–4292.
- (3) Higgs, D. E.; Nelen, M. I.; Detty, M. R. *Org. Lett.* **2001**, *3*, 349–352.
- (4) Butcher, T. S.; Detty, M. R. *J. Org. Chem.* **1999**, *64*, 5677–5681.
- (5) Abe, M.; Detty, M. R.; Gerlits, O. O.; Sukumaran, D. K. *Organometallics* **2004**, *23*, 4513–4518.
- (6) Zhang, B.; Hou, W.; Ye, X.; Fu, S.; Xie, Y. *Adv. Funct. Mater.* **2007**, *17*, 486–492.
- (7) Manna, L.; Milliron, D. J.; Meisel, A.; Scher, E. C.; Alivisatos, A. P. *Nat. Mater.* **2003**, *2*, 382–385.
- (8) Chu, J.; Li, X.; Xu, P. *J. Mater. Chem.* **2011**, *21*, 11283–11287.
- (9) Gamboa, S. A.; Sebastian, P. J.; Mathew, X.; Nguyen-Cong, H.; Chartier, P. *Sol. Energy Mater. Sol. Cells* **1999**, *59*, 115–124.
- (10) Smith, A. M.; Nie, S. *Acc. Chem. Res.* **2010**, *43*, 190–200.
- (11) Narita, Y.; Hagiri, I.; Takahashi, N.; Takeda, K. *Jpn. J. Appl. Phys. I* **2004**, *43*, 4248–4258.
- (12) Narita, Y.; Takeda, K. *Jpn. J. Appl. Phys. I* **2006**, *45*, 2628–2642.
- (13) Muranaka, A.; Yasuie, S.; Liu, C. Y.; Kurita, J.; Kakusawa, N.; Tsuchiya, T.; Okuda, M.; Kobayashi, N.; Matsumoto, Y.; Yoshida, K.; Hashizume, D.; Uchiyama, M. *J. Phys. Chem. A* **2009**, *113*, 464–473.
- (14) McCullough, R. D.; Kok, G. B.; Lerstrup, K. A.; Cowan, D. O. *J. Am. Chem. Soc.* **1987**, *109*, 4115–4116.
- (15) Bendikov, M.; Wudl, F.; Perepichka, D. F. *Chem. Rev.* **2004**, *104*, 4891–4946.
- (16) Wudl, F.; Aharon-Shalom, E. *J. Am. Chem. Soc.* **1982**, *104*, 1154–1156.
- (17) Millefiori, S.; Alparone, A. *Phys. Chem. Chem. Phys.* **2000**, *2*, 2495–2501.
- (18) Jansik, B.; Schimmelpfennig, B.; Norman, P.; Macak, P.; Agren, H.; Ohta, K. *THEOCHEM* **2003**, *633*, 237–246.
- (19) Welch, G. C.; Coffin, R.; Peet, J.; Bazan, G. C. *J. Am. Chem. Soc.* **2009**, *131*, 10802–10803.
- (20) Job, A.; Wakamiya, A.; Kehr, G.; Erker, G.; Yamaguchi, S. *Org. Lett.* **2010**, *12*, 5470–5473.
- (21) Welch, G. C.; Bazan, G. C. *J. Am. Chem. Soc.* **2011**, *133*, 4632–4644.
- (22) Shultz, A. M.; Farha, O. K.; Hupp, J. T.; Nguyen, S. T. *Chem. Sci.* **2011**, *2*, 686–689.
- (23) Wang, B.; Wasielewski, M. R. *J. Am. Chem. Soc.* **1997**, *119*, 12–21.
- (24) Thomas, S. W.; Joly, G. D.; Swager, T. M. *Chem. Rev.* **2007**, *107*, 1339–1386.
- (25) Kappaun, S.; Scheiber, H.; Trattnig, R.; Zojer, E.; List, E. J. W.; Slugovc, C. *Chem. Commun.* **2008**, 5170–5172.
- (26) Yang, R.; Wu, H.; Cao, Y.; Bazan, G. C. *J. Am. Chem. Soc.* **2006**, *128*, 14422–14423.
- (27) Yang, R.; Garcia, A.; Korystov, D.; Mikhailovsky, A.; Bazan, G. C.; Nguyen, T. Q. *J. Am. Chem. Soc.* **2006**, *128*, 16532–16539.
- (28) McCullough, J. D. *Inorg. Chem.* **1975**, *14*, 2285–2286.
- (29) Jahnke, A. A.; Howe, G. W.; Seferos, D. S. *Angew. Chem., Int. Ed.* **2010**, *49*, 10140–10144.
- (30) Cook, T. R.; Esswein, A. J.; Nocera, D. G. *J. Am. Chem. Soc.* **2007**, *129*, 10094–10095.
- (31) Cook, T. R.; Surendranath, Y.; Nocera, D. G. *J. Am. Chem. Soc.* **2009**, *131*, 28–29.
- (32) Lee, C. H.; Cook, T. R.; Nocera, D. G. *Inorg. Chem.* **2011**, *50*, 714–716.
- (33) Teets, T. S.; Nocera, D. G. *J. Am. Chem. Soc.* **2009**, *131*, 7411–7420.
- (34) Sweat, D. P.; Stephens, C. E. *Synthesis* **2009**, 3214–3218.
- (35) Davies, A. G.; Schiesser, C. H. *J. Organomet. Chem.* **1990**, 389, 301–313.
- (36) Potapov, V. A.; Amosova, S. V.; Doron'kina, I. V. *Chem. Heterocycl. Compd.* **2002**, *38*, 259–260.
- (37) Potapov, V. A.; Amosova, S. V.; Doron'kina, I. V.; Zinchenko, S. V. *Sulfur Lett.* **2001**, *24*, 275–279.
- (38) **Caution:** Diacetylene gas is formed and is flammable and can form explosive mixtures with air. Care should be taken with the deprotection of bis(trimethylsilyl)butadiyne.
- (39) Sweat, D. P.; Stephens, C. E. *J. Organomet. Chem.* **2008**, 693, 2463–2464.
- (40) Mack, W. *Angew. Chem., Int. Ed. Engl.* **1966**, *5*, 896–896.
- (41) Rhoden, C. R. B.; Zeni, G. *Org. Biomol. Chem.* **2011**, *9*, 1301–1313.
- (42) Inoue, S.; Jigami, T.; Nozoe, H.; Otsubo, T.; Ogura, F. *Tetrahedron Lett.* **1994**, *35*, 8009–8012.
- (43) Promarak, V.; Punkvuang, A.; Jungsuttiwong, S.; Saengsuwan, S.; Sudyoadsuk, T.; Keawin, T. *Tetrahedron Lett.* **2007**, *48*, 3661–3665.
- (44) Takimiya, K.; Konda, Y.; Ebata, H.; Niihara, N.; Otsubo, T. *J. Org. Chem.* **2005**, *70*, 10569–10571.
- (45) Detty, M. R.; Friedman, A. E.; McMillan, M. *Organometallics* **1994**, *13*, 3338–3345.
- (46) Beaujuge, P. M.; Amb, C. M.; Reynolds, J. R. *Acc. Chem. Res.* **2010**, *43*, 1396–1407.
- (47) Detty, M. R.; Frade, T. M. *Organometallics* **1993**, *12*, 2496–2504.
- (48) Detty, M. R.; Friedman, A. E. *Organometallics* **1994**, *13*, 533–540.
- (49) Engman, L.; Lind, J.; Merenyi, G. *J. Phys. Chem.* **1994**, *98*, 3174–3182.
- (50) Detty, M. R.; Luss, H. R. *J. Org. Chem.* **1983**, *48*, 5149–5151.
- (51) Detty, M. R.; Lenhart, W. C.; Gassman, P. G.; Callstrom, M. R. *Organometallics* **1989**, *8*, 866–870.
- (52) Detty, M. R.; Luss, H. R.; McKelvey, J. M.; Geer, S. M. *J. Org. Chem.* **1986**, *51*, 1692–1700.
- (53) Lee, S. H.; Nakamura, T.; Tsutsui, T. *Org. Lett.* **2001**, *3*, 2005–2007.
- (54) Chen, C. H.; Hsieh, C. H.; Dubosc, M.; Cheng, Y. J.; Hsu, C. S. *Macromolecules* **2010**, *43*, 697–708.
- (55) Frisch, M. J., et al. *Gaussian 09*, revision A.1; Gaussian, Inc.: Wallingford, CT, 2009.
- (56) Becke, A. D. *J. Chem. Phys.* **1993**, *98*, 5648–5652.
- (57) Becke, A. D. *J. Chem. Phys.* **1996**, *104*, 1040–1046.
- (58) Hay, P. J.; Wadt, W. R. *J. Chem. Phys.* **1985**, *82*, 270–283.
- (59) Bauernschmitt, R.; Ahlrichs, R. *Chem. Phys. Lett.* **1996**, *256*, 454–464.